Available online at www.sciencedirect.com
SCIENCE DIRECT®
Polymer 45 (2004) 3257–3265
polymer
www.elsevier.com/locate/polymer

Hybrid ternary organic–inorganic films based on interpolymer complexes and silica

Yadienka Martínez[a], Jaime Retuert[a,*], Mehrdad Yazdani-Pedram[b], Helmut Cölfen[c,*]

[a]*Center for Advanced Interdisciplinary Research in Materials (CIMAT) and Facultad de Ciencias Físicas y Matemáticas, Universidad de Chile, Av. Beaucheff 850, Casilla 2777, Santiago, Chile*

[b]*Center for Advanced Interdisciplinary Research in Materials (CIMAT) and Facultad Ciencias Químicas y Farmacéuticas, Universidad de Chile, Olivos 1007, Casilla 233, Santiago, Chile*

[c]*Max-Planck Institute of Colloids and Interfaces, Colloid Chemistry, Research Campus Golm, Am Mühlenberg, D-14424 Potsdam, Germany*

Received 23 October 2003; received in revised form 2 March 2004; accepted 11 March 2004

Abstract

Homogeneous transparent hybrid films consisting of chitosan (CHI), poly(monomethyl itaconate) (PMMI) and silica were obtained indicating the absence of microphase separation. These ternary hybrid materials are very interesting since materials with high functionality can be obtained presenting different properties from those of the starting materials but with the advantage of preserving the inherent property of each component. The inorganic phase was prepared by sol–gel process of tetraethoxysilane (TEOS). Most of the amine groups from CHI (pK_b 7.7) are quaternized in the acidic medium used in the preparations (pH = 2), where a physical crosslinking via hydrogen bonding could occur through carboxyl groups from PMMI. Silica gel obtained from TEOS has been intercalated as a very fine dispersion in the polymer complex formed between CHI and PMMI. Transmission electron microscopy and atomic force microscopy was used to examine the homogeneity of the ternary polymer hybrids (CHI/PMMI/SiO_2), obtained as self-supported films. The results support the nanometer scale dispersion of the phases. Porous silica films with high BET area were obtained by calcination of the hybrid films. The mean pore diameter of these silica films corresponds to the dimension of the polymer domains observed in the pristine hybrid films. Moreover, it was found that the swelling behavior of the samples was influenced by the organic and inorganic phases, where the inorganic phase tends to diminish the swelling.

Keywords: Chitosan; Hybrid films; Interpolymer complex

1. Introduction

The sol–gel process is a well-know technique for forming organic–inorganic materials [1–6]. Using this method, a network-forming precursor sol and organic compounds can be combined to develop materials with attractive properties, in particular good optical, mechanical and thermal properties as well as chemical stability. These hybrid materials are characterized by compatibility at a submicroscopic level of organic components with inorganic oxides. Alkoxysilane monomers are commonly used as inorganic network forming reagents that are first transformed into soluble polymeric species by controlled hydrolysis and condensation reactions catalyzed by acid or base. At this point, it is possible to mix the inorganic component with the organic one to obtain hybrid materials at room temperature. The resulting composites can be prepared with different physical forms such as films, monoliths, etc. [7–9] and they are attractive candidates for optical devices, separation media, catalyst supports, microelectronic coatings, sensor coatings and structural materials [10].

Incorporation of organic polymers, especially those with amino or amide groups, allows the formation of molecular hybrids often stabilized by strong hydrogen bonding. Polymers such as chitosan (CHI) are able to form hybrids with silica gel by using this method [11]. The resulting binary hybrid composites have been obtained as transparent flexible films despite of high silica content indicative of silica particle sizes beyond the wavelength of visible light

* Tel.: +56-2-6784226; fax: +56-2-6994119.
E-mail addresses: jretuert@dqb.uchile.cl (J. Retuert), coelfen@mpikg-golm.mpg.de (H. Cölfen).

0032-3861/$ - see front matter © 2004 Elsevier Ltd. All rights reserved.
doi:10.1016/j.polymer.2004.03.046

[11]. It is also known that the amino side group of chitosan is responsible for its polycationic character and the formation of well-known intermolecular complexes with carboxylic and polycarboxylic acids [12–14].

In this work chitosan and poly(monomethyl itaconate) (PMMI) were used for the first time as organic polymers to obtain silica-based ternary hybrid films by the sol–gel technique. The addition of PMMI as an anionic polyelectrolyte to the binary system CHI/SiO_2 has been done in order to modify the physical and mechanical properties of these films because new interactions are generated. To our best knowledge, ternary hybrid nanocomposites with high degree of compatibility, especially in the form of self-supported films, have not been reported in the literature. These ternary hybrid materials are very interesting since materials with high functionality can be obtained presenting different properties from those of the starting materials but with the advantage of preserving the inherent property of each component. The introduction of the organic groups in the inorganic network originates new structural properties and therefore promotes new applications for the resulting composite material such as functional coating by introducing ions and/or small molecules.

Several compositions were prepared and analyzed to find the compatibility limit of the three components and to evaluate the formation of a polycomplex system in which it is possible to grow the inorganic phase.

2. Experimental

Chitosan (high molecular weight) purchased from Aldrich, (Milwaukee, USA), was purified by extraction with acetone in a Soxhlet for 24 h and dried under vacuum at room temperature to constant weight. The degree of deacetylation and molecular weight were determined according to the procedures described by Rinaudo and Domard [15]. The degree of deacetylation was estimated as 83% and the weight average molecular weight was determined as 3.55×10^5 g mol^{-1} by combined viscosity-light scattering measurements. CHI was used as a 1% solution in dilute formic acid (5%) (pH 1.8). In order to obtain a siloxane sol, a solution of tetraethoxysilane (TEOS) (Aldrich) in ethanol (Aldrich) was hydrolyzed with an aqueous solution of formic acid diluted in ethanol in order to have a molar composition TEOS:H_2O:Formic acid:EtOH = 1:1:0.01:10. This solution was kept at 50 °C in an open container during 1 day.

Monomethyl itaconate was prepared by reaction of itaconic acid with methanol under fairly acidic conditions by the method described by Baker et al. for lower monoesters [16]. The pure monomer was obtained by dissolving the reaction products in cool chloroform, filtration and precipitation in n-hexane (melting point, 69–70 °C). PMMI was obtained by radical polymerization in bulk under N_2 at 75 °C in the presence of 0.2 mol% of azobisisobutyronitrile as radical initiator. PMMI was purified by repeated dissolution in methanol and precipitation in diethyl ether. The apparent number and weight average molecular weight ($\bar{M}_n = 1.1 \times 10^5$ g mol^{-1}, $\bar{M}_w = 1.6 \times 10^5$ g mol^{-1}) was determined by gel permeation chromatography (GPC) by using a Waters 600 HPLC fitted with a Shodex 803 column and a differential refractive index detector. Water containing 0.1 M NaCl was used as eluent with a flow rate of 1 ml/min. Column calibration was performed by using Pullulan standard samples.

2.1. Film preparation

Siloxane sol and PMMI ethanol solutions were mixed in the appropriate ratios and stirred for 30 min. Then CHI solutions were incorporated and the mixture was stirred for 24 h. For all the compositions the pH values of the mixtures were around 2.7–2.75. The SiO_2:CHI:PMMI molar ratio of the samples was calculated from the molecular weight of the monomeric unit of CHI (168.1 g mol^{-1}) considering the acetylation degree of 17% and the molecular weight of the PMMI repeating unit (144 g mol^{-1}). Films of 15–20 μm thickness were obtained by solution casting on a polypropylene film and by letting the solvent to evaporate at room temperature. Thicker membranes of 140–145 μm were obtained by depositing the hybrid solution in a polystyrene petri-dish.

2.2. Characterization of the hybrid films

Thermogravimetric analysis was performed in a thermal analyzer NETZSCH TG209, in the temperature range from 20 to 900 °C at a heating rate of 20 °C/min, under nitrogen. Membranes were first dried in a vacuum oven at 70 °C for 2 days. Differential scanning calorimetry was performed in a TA Instruments 2910 MDSC thermal analyzer. About 10 mg of sample were heated at 10 °C/min under nitrogen from 25 to 250 °C.

The samples were analyzed in an infrared Fourier transform spectrophotometer, Nicolet 520 FT-IR, in the region from 4000 to 400 cm^{-1}. A commercial atomic force microscopy (AFM) (Nanoscope III, Digital Instruments) was used to perform the surface analysis of the hybrid films operating in tapping mode. For the purpose of comparison, the root mean square roughness (RMS) was chosen to characterize the topography of the films. Transmission electron microscopy (TEM) was used to investigate the structure of the hybrid films. The samples were prepared by thin-slicing the film at a thickness of ca. 100 nm with a Leica ultracut UCT ultramicrotome and placing them on a copper TEM grid. A DMS 940 A (Carl Zeiss, Jena) microscope was used. The specific surface area (S_{Bet}), mean pore diameter (ϕ) and specific desorption pore volumes of samples calcined at 700 °C were determined by nitrogen physisorption at 77 K using a Micromeritics ASAP 2010

sorptometer (Micromeritics Instrument Corporation, USA). Samples were degassed for 2 h at 200 °C and 0.1 Pa prior to measurement. All calculations were performed using the associated Micromeritics software.

2.3. Swelling experiments

The swelling behavior was measured by immersing pre-weighed dry samples of about 200–250 mg in pH 4 and pH 9 solutions at 37 °C. The water uptake was calculated by measuring the weight gain of the samples at a given time interval. Excess surface water was blotted out with filter paper before weighing. The weight degree of swelling (W_{Sd}) was calculated using the following equation:

$$W_{sd}(\%) = \frac{W_s - W_d}{W_d} 100$$

where, W_s and W_d denote the weight of the swollen and dry samples, respectively.

3. Results and discussion

The hydrolysis of TEOS using acid catalysts, in the presence of little water, mainly produced linear polysiloxanes [17], then the resulting sol is only weakly branched. Film formation should be favored under these conditions. The molecular structure of CHI and PMMI are given in Scheme 1. It is expected that the functional groups present in these polymers should allow an interaction at molecular level with the inorganic component and therefore the formation of hybrid film should be possible.

Table 1 shows the different compositions studied, where these are expressed as molar ratios. Transparent homogeneous films were obtained for all the compositions, indicating no phase separation of the organic and inorganic phases at a scale smaller than the wavelength of visible light, that is 400 nm.

While PMMI/CHI forms transparent films in a wide composition range, hybrid transparent films of SiO_2/PMMI can not be obtained. PMMI has polar functional groups that could interact with residual silanol groups of silica gel through hydrogen bonding. However, phase separation was observed for a wide range of compositions. It is worth to mention that SiO_2/CHI systems form transparent films only

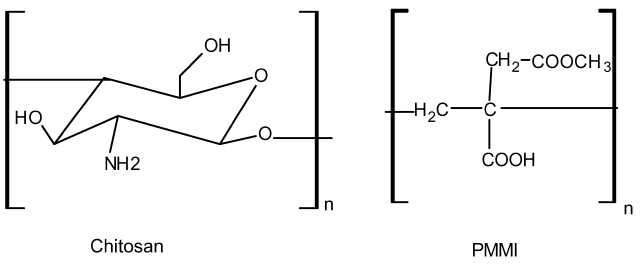

Scheme 1. Chemical structure of chitosan and PMMI.

Table 1
Macroscopic properties of the hybrid films with different compositions. T (transparent) F (flexible) and B (brittle)

Sample	CHI:SiO_2:PMMI	Properties
CP	1:0:0.5	F,T
CSP1	0.6:1:0.3	F,T
CSP2	0.6:1:0.6	F,T
CSP3	1:0.7:0.5	F,T
CSP4	1:0.1:0.5	F,T
CSP5	0.4:1:0.5	B,T
CSP6	0.3:1:0.5	B,T
CSP7	0.3:1:0.6	B,T
CSP8	0.1:1:0.1	B,T
SP	0:1:1	Phase separation

when a silanol sol of certain characteristics is used as SiO_2 source [11]. Nevertheless, in this work silanol sols obtained with different acid catalysts (formic acid) and reaction times have been tested. In all cases, transparent films where produced, indicating a better compatibility of this system with the inorganic component.

Films prepared with the binary system CHI/SiO_2 with different compositions, were easily disintegrated in water but the ternary films kept unaltered likely due to the polyelectrolyte complex formation between CHI and PMMI. The apparent flexibility of these films was observed to depend on the SiO_2 and PMMI content. Films with and without silica were observed to strongly adhere to glass and on graphite surfaces. This new coating property could be potentially important for multiple applications such as fixation of chemical sensor elements for electrodes and the formation of thin films on substrates with variety of shapes.

3.1. FT-IR analysis

Fig. 1(A) shows the infrared spectra for the pure components and the hybrid film CHI/SiO_2/PMMI with molar ratio (r) 0.6:1:0.6. For comparison purposes, a chitosan film was prepared by casting the precursor solution. The region from 2000 to 350 cm^{-1} is shown in detail. The main absorption bands of CHI, 1658 cm^{-1} (amide I) and 1595 cm^{-1} ($-NH_2$ bending) appears in the CHI film as one signal at 1582 cm^{-1}. The absorption bands at 1154 cm^{-1} (anti-symmetric stretching of C–O–C bridge), 1078 and 1032 cm^{-1} (skeletal vibrations involving the C–O stretching) are characteristic of its saccharide structure [18]. On the other hand, PMMI exhibits the characteristic absorption band at 1734 cm^{-1} due to the C=O stretching vibrations. The spectrum of SiO_2 shows peaks at 1085 and 795 (Si–O–Si asymmetric and symmetric bond stretching vibration, respectively) and at 950 cm^{-1} (Si–OH stretching) [19].

The main absorption bands of PMMI and SiO_2 are present in the spectra of the hybrid films. The most important change is the displacement of the carbonyl absorption band of PMMI (1734 cm^{-1}) to lower frequencies ($\approx$15 cm^{-1}) in all the samples. This could indicate the role

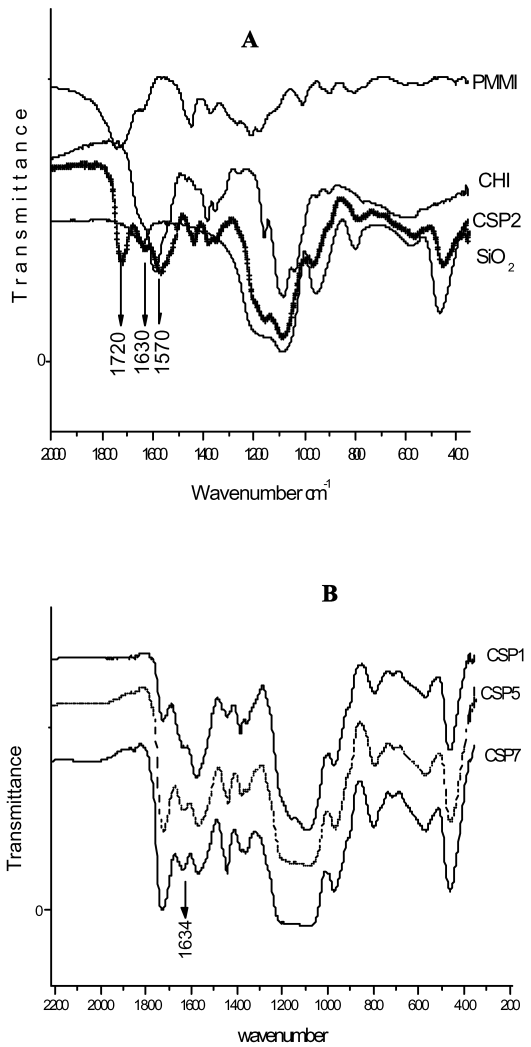

Fig. 1. (A) Infrared spectra for CHI, PMMI, SiO_2 and hybrid film CSP2. (B) Infrared spectra for hybrid film CSP1,5,7.

of the carboxyl groups in the compatibilization of the system components probably through hydrogen bonding. The characteristic signals of SiO_2 appear at 1089, 967 and 786 cm^{-1}. These IR peaks confirm the formation of structural units of Si–O–Si in the hybrid films. It is worth to mention that the Si–OH absorption band shows a displacement to higher frequencies. Another important change is the band at 1634 cm^{-1} that it is not present in the spectra of the starting polymers or even in their physical mixture. As can be seen in Fig. 1(B) the intensity of this absorption band increases with the amount of PMMI incorporated. This peak suggests the existence of a specific interaction between chitosan and PMMI what is indicative of complexation between the amino groups of chitosan and the carboxyl groups of PMMI [20].

The proton-polyion interaction for PMMI was studied by the determination of the Eisenberg interaction parameter (f^*) by means of electrical conductivity measurements in water [21]. This parameter is defined as $f^* = \Lambda_{exp}/\Lambda_{teo}$ where Λ_{exp} is the experimental equivalent conductivity of the polyion solution and Λ_{teo} is the polyion equivalent conductivity that can be calculated using the Manning's theory [22]. f^* is directly related to the degree of dissociation and therefore it will be possible to estimate the extension of PMMI dissociation in order to know if electrostatic or hydrogen bonding interactions are responsible for the polyelectrolyte complex formation.

Fig. 2 left shows the Kohlrausch plot for PMMI solution and Fig. 2 right presents the f^* behavior for PMMI. As can be seen f^* has a very low value and remains almost constant over the investigated concentration range. This fact indicates that PMMI is almost completely in the undissociated form and then no electrostatic interactions are present. This could indicate that hydrogen-bonding interactions should be responsible of the complex formation.

As CHI provides amine groups, which can be quaternized almost completely at pH 2 (pK_b 7.7) [23], a physical crosslinking with PMMI via hydrogen bonding can be obtained through carboxyl groups from PMMI once the formic acid was evaporated during the film formation. This has been previously observed for the system poly(acrylic acid)/chitosan polyelectrolyte complex [24].

In CHI/SiO_2 hybrid films it has been established that the formation of hydrogen bonding between residual amide

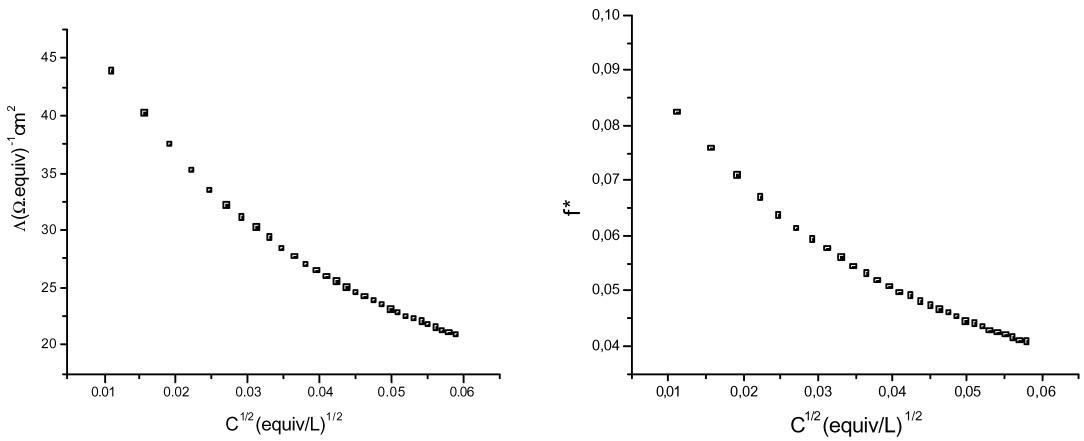

Fig. 2. Equivalent conductivity versus $C^{0.5}$ (left) and f^* versus $C^{0.5}$ (right) for PMMI in water.

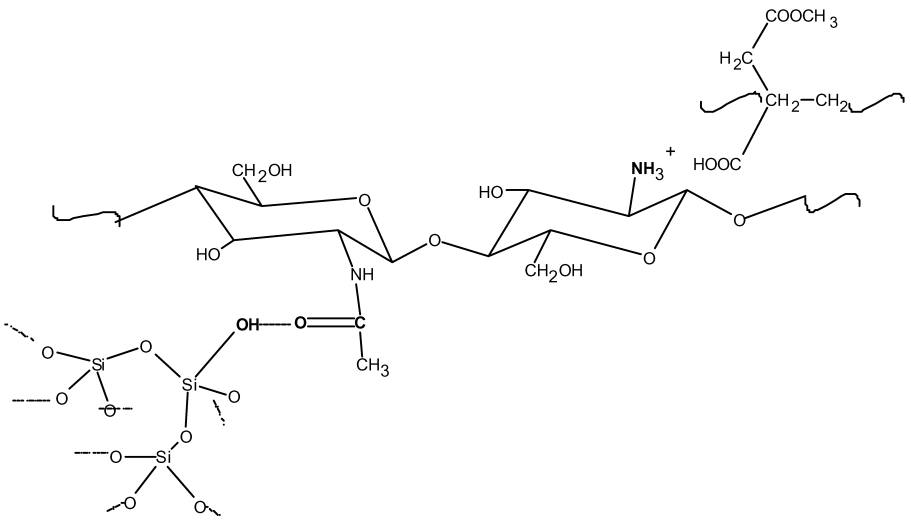

Scheme 2. Proposed interactions of SiO_2, CHI and PMMI in hybrid films.

groups of chitosan and silanol groups are responsible for the compatibility of the two components [11]. In our case the interactions represented in Scheme 2 are proposed as the main interactions responsible for the compatibility of the phases observed in the ternary system.

The improvement of the compatibility of the three components in the hybrid samples was speculatively caused by the increased interactions at the interfaces CHI–SiO_2 and SiO_2–PMMI, where CHI should act as a compatibilizer. As was mentioned above, PMMI does not form transparent hybrid films with silica in binary combinations because of phase separation. However, interactions like those shown in Scheme 2 allow a homogeneous incorporation of PMMI into the CHI/SiO_2 system due to the proposed role of CHI as a compatibilizer with respect to silica and PMMI phases.

3.2. Thermal characterization of the hybrid films

Fig. 3 shows the differential thermogravimetric curves obtained for pure CHI, CHI/PMMI and hybrid films of different compositions. The differential thermogravimetric curve of PMMI shows a maximum decomposition at 170 °C (not shown) as a result of decarboxylation of the polymer [25]. The two decomposition temperatures of the main stages of mass loss for the samples are shown in Table 2. The percentage of silica content is also presented in Table 2. This was calculated considering that the entire precursor has reacted forming silicon dioxide.

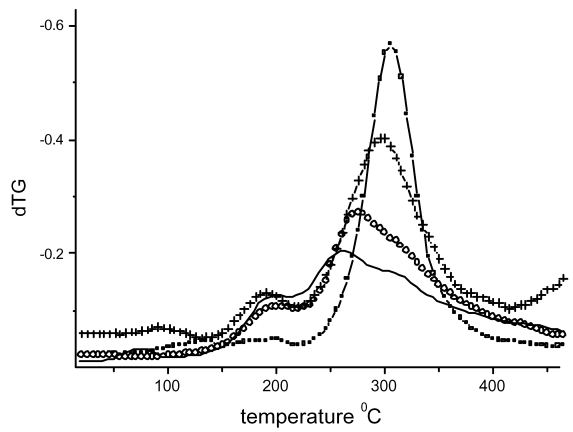

Fig. 3. Differential thermogravimetric curve obtained for CHI (■) CP (+) CSP1 (○) and CSP6 (–) under N_2.

The first decomposition stage has a maximum at 193–200 °C depending on the sample and it's absent in the thermogram of CHI. It has been reported [13] that amide bond formation in chitosan-acrylic acid salts occurs appreciably at 100 °C. This reaction results from the modification of polyelectrolyte complex membranes of chitosan and polyacrylic acid by heating at 180 °C for 1 h. Interestingly, the temperature for the first decomposition in the hybrid films is higher than that for the decarboxylation of PMMI. This could be the result of dehydration of the interpolyelectrolyte complex between CHI and PMMI, eventually leading to the formation of interchain amide bonds. Degradation of some unreacted COOH groups of PMMI can also contribute to the total weight loss observed in this degradation stage.

The thermogram of chitosan exhibits a decomposition pattern with a maximum at 306 °C. This temperature is about 9 °C lower in CHI/PMMI films. The incorporation of the inorganic oxide also seems to promote the thermal degradation of the material. The main stages of mass loss occur at lower temperatures (about 20–40 °C lower) with the increase of the SiO_2 and PMMI concentration in the hybrid, indicating increased thermal instability of the polymer as the result of complexation. Other authors have reported this behavior in polyelectrolyte complexes and in SiO_2 based hybrid composites [26,27].

The DSC thermogram of the sample CSP-7 (Fig. 4) shows two exothermic processes in the heating curve both associated to a mass loss (not shown). No signals were observed in the second heating curve. This indicates that no

Table 2
Temperature at the maximum of the main stages of mass loss ($T1$) and ($T2$) and percentage of SiO_2 (calculated) for hybrids of different composition

Sample	$T1$ (°C)	$T2$ (°C)	SiO_2 (%)
CHI		306	0
CP	193	295	0
CSP1	199	271	30.1
CSP2	200	279	24.7
CSP3	198	284	15.4
CSP4	199	284	2.6
CSP5	199	280	30.6
CSP6	199	260	33.4
CSP7	197	280	30.9

order–disorder arrangement occurred when heating the sample to 200 °C. In this way the differences in the above curves were only due to sample decomposition (197 °C for CP7 according to Table. 1) and/or solvent evaporation at the lower temperature accompanied by densification of the film structure.

3.3. AFM

The surface analysis of the hybrid films was performed by AFM. A typical AFM height image of the samples is presented in Fig. 5 top. The surface appears to be free of visible defects and is very smooth. For samples CSP1 and CSP5 average roughness values (RMS) of 0.436 and 0.443 nm were observed.

The phase contrast picture (Fig. 5 bottom) shows a homogeneous surface indicating either that the silica particles are located in the interior of the film or that the surface of the film is composed of silica to a significant part so that no localized areas of soft and hard material could be observed.

3.4. TEM analysis

Ultrathin films were cut by microtoming and observed in a transmission electron microscope. Fig. 6 top shows the TEM images of the sectioned sample. A homogeneous distribution of intimately associated black silica nanoparticles of about 2–2.5 nm is observed.

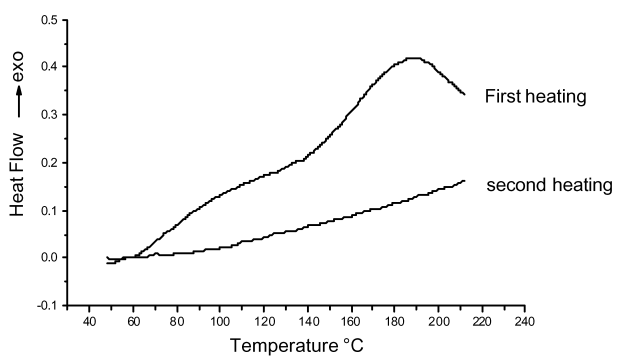

Fig. 4. DSC thermogram obtained for sample CSP-7.

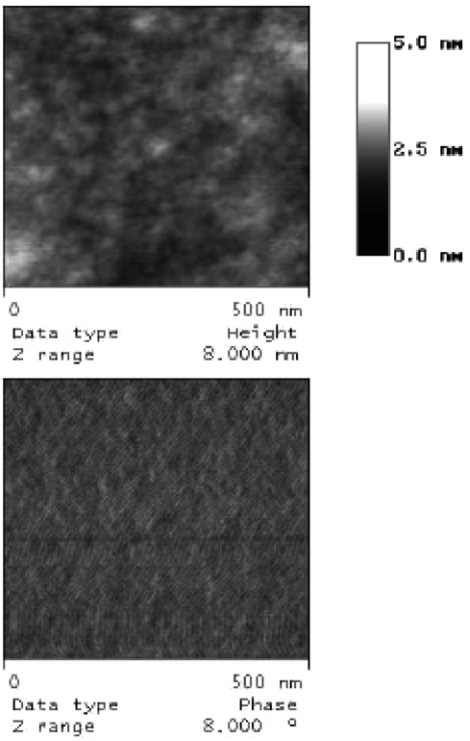

Fig. 5. AFM image of the surface of hybrid film CSP5. Top: surface topology. Bottom: phase contrast.

The organic components are more or less homogeneously distributed as is apparent by the film transparency and in addition, the included silica particles must be dispersed on length scales below that of the visible light wavelength. Nevertheless, Fig. 6 top reveals their low particle size but also shows a slightly inhomogeneous distribution of the silica particles with a higher electron density compared to the invisible polymer complex.

Fig. 6 bottom shows a TEM image of the film after calcination. The silica particles are joined forming domains with the removal of the organic phase producing in this way a denser film. Silica nanoparticles of about 2.5–3 nm are observed and a porous material results.

The silica films are transparent and very fragile. This indicates that the calcined film is also homogeneous at least on the length scale of visible light and that no larger inhomogeneous domains than 400 nm exist. Combined with the information of Fig. 6 bottom, this means that although a slight silica inhomogeneity exists inside the films, the domain interfaces are not sharp so that transparent films are obtained.

3.5. Nitrogen porosimetry study

In Table 3 the specific surface areas, as well as porosity values and characteristics of the micropore structure are presented for porous silica films prepared starting from hybrid films with different compositions. As can be seen, these films are mesoporous but contain a considerable

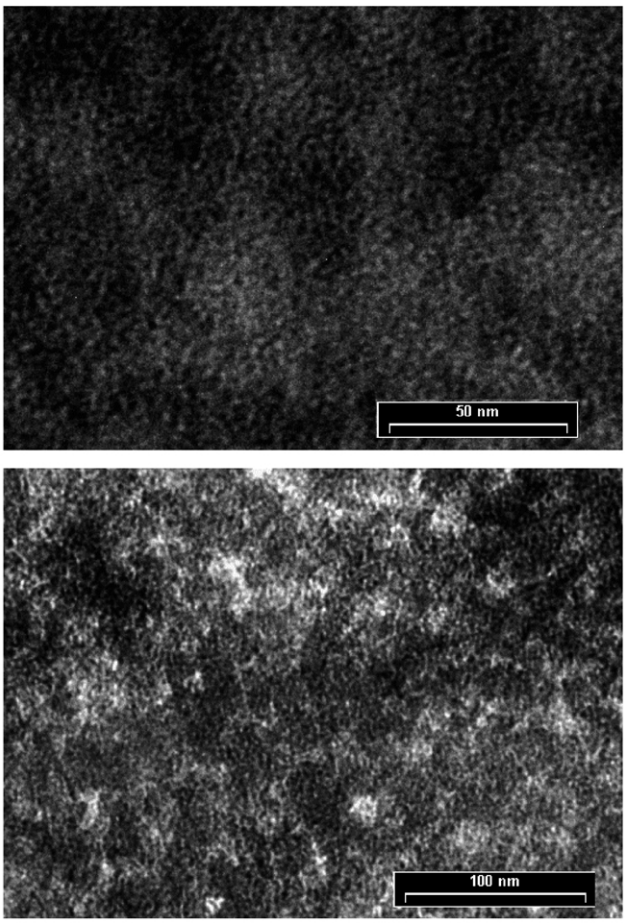

Fig. 6. TEM image of CSP6 CHI:SiO_2:PMMI (0.3:1:0.5) hybrid film before calcination (top) and after calcination (bottom).

micropore area. However, the mean pore diameter corresponds closely to the dimensions of the polymer component phase observed in the TEM micrographs (Fig. 6 bottom). This fact also confirms the molecular dispersion of the combined phases [28].

Moreover, in all cases the adsorption isotherms (Fig. 7) correspond to the type IV curves with a H2 hysteresis at P/P_0 of ~0.4–0.8. There is a well defined plateau following the loop at $P/P_0 > 0.8$ suggesting the occurrence of pore filling by capillary condensation of nitrogen in the framework-confined mesopores instead of adsorption in the interparticle textural pores [29].

Table 3
Pore volume and surface area of porous silica films obtained by calcinating the hybrid films

Sample	S_{Bet} (m^2/g)	Pore volume (cm^3/g)	Pore ϕ BJH (Å)	Micropore	
				Area (m^2/g)	Volume (cm^3/g)
CSP1	449	0.227	32	134	0.058
CSP3	553	0.673	54	52	0.016
CSP6	599	0.430	33	50	0.016

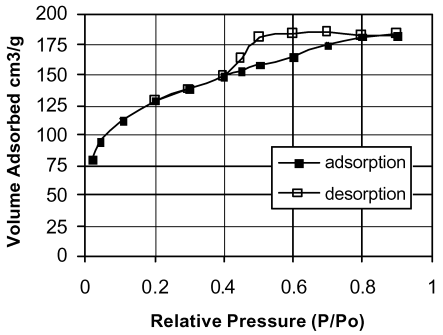

Fig. 7. Absorption isotherm obtained for sample CSP1.

3.6. Swelling behavior

Electrostatic interactions between macromolecular chains take an important role in swelling properties. Generally, the volume of an ionic gel is assumed to be determined by a balance of two pressures. One is the ion swelling pressure or osmotic pressure, which is due to the difference in mobile ion concentrations between the gel and the external solution. The other is the network swelling pressure that tends to keep the gel volume constant [30].

The swelling equilibrium is defined by a minimum of the free energy so that the difference of the solvent chemical potential in the two coexisting phases $\Delta\mu_1$ is zero [31]:

$$0 = \Delta\mu_1 = \Delta\mu_{1,M} + \Delta\mu_{1,El} + \Delta\mu_{1,Ion}$$

with the mixing term:

$$\Delta\mu_{1,M} = RT(\ln\phi_1 + \phi_2 + \chi\phi_2^2)$$

the network term:

$$\Delta\mu_{1,El} = \nu^* RTV_{01}\eta\phi_2^{1/3}$$

and the ionic term

$$\Delta\mu_{1,Ion} = 2RTV_{01}\left[c_s - \sqrt{\left\{c_s^2 + \left(\frac{\rho\phi_2}{2M_2}\right)^2\right\}}\right]$$

with R = gas constant, T = thermodynamic temperature, ϕ = volume fraction with index 1 = solvent, 2 = polymer, χ = Flory–Huggins interaction parameter, ν^* = number of elastically active network chains per dry unit volume, η = mean square end-to-end distance, A = numerical factor, c_s = salt concentration, ρ = density of the dry polymer and M_2 = molar mass of the polymer per free monovalent counterion.

Fig. 8 shows the variation of the water uptake (W_{sd}) as a function of time at pH 9 (8a) and pH 4 (8b) for hybrid samples of different compositions, including a sample without SiO_2 (CP). The water sorption kinetics shows that at pH 4 the water content at equilibrium was reached in the first couple of minutes, but at pH 9 samples richer in PMMI show a time dependency of the swelling process. It can also be observed that there is an appreciable dependency of W_{sd} with the composition. Table 4 shows these results.

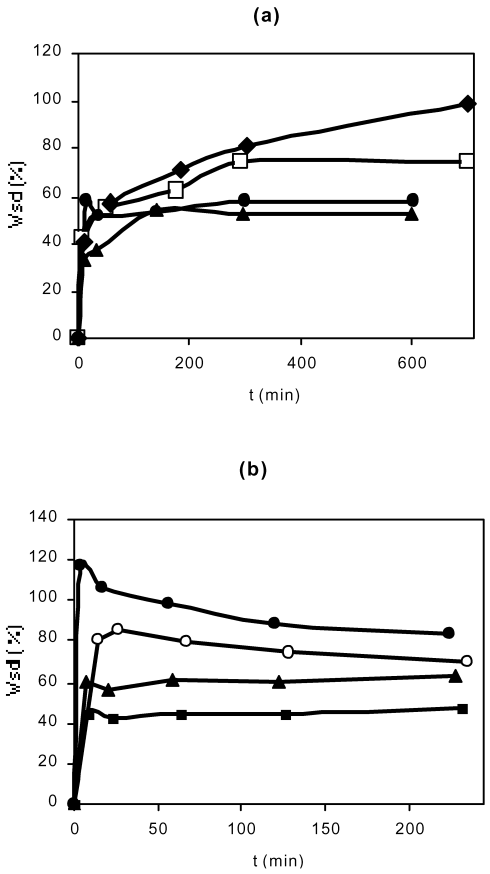

Fig. 8. Water sorption isotherms for (a): CSP2 (▲), CSP3 (●), CSP5 (□) and CSP7 (◆) at pH 9 and (b): CSP2 (■), CSP1 (▲), CSP3 (○) and CP (●) at pH 4 and 37 °C.

A very fast swelling was observed in samples with the greater CHI content at acidic pH, reaching in few minutes its maximum, which however decreases by longer contact time. The quick response of the hydrogel can be attributed to a fast protonation of the amine groups of the CHI. In this case, the interaction of the NH_3^+ groups with carboxyl groups of PMMI chains could lead to a closed structure that would allow to host a great amount of acid solution, which at longer contact times could diffuse to the exterior until reaching the equilibrium. A similar behavior has been observed in other CHI based hydrogels [32].

Due to the hybrid nature of the samples, W_{sd} is not only influenced by the organic phase but also by the inorganic component, which in general tends to diminish the swelling of the system. Films richer in PMMI exhibited higher swelling at high pH and those richer in CHI at lower pH values as seen in Table 4.

Table 4
Variation of W_{sd} (%)$_\infty$ with composition and pH

Sample	W_{sd} (%)$_\infty$ pH 4	pH 9
CP	95.9	100
CSP1	64.6	40.1
CSP2	46.2	52.7
CSP3	70.6	58.1
CSP5	–	73.8
CSP6	–	89.5
CSP7	–	98.5

At an alkaline pH amino groups of chitosan are neutralized, while the carboxyl groups of PMMI remain negatively charged, the complex gel becomes negatively charged and the gel takes up mobile cations from the external solution. At pH 4 the carbonyl groups are neutralized and the amino groups are positively charged, where the latter determine flow of mobile ions to the gel. Thus, swelling occurs due to the increase in the osmotic pressure of the complex gel. As expected, films with higher content of SiO_2 show the lowest swelling due to the more rigid structure associated with the SiO_2 matrix (see Fig. 8).

These results confirm the formation of the polyelectrolyte complex between CHI and PMMI and the molecular interaction engaged in this structure with the inorganic component. All components have an influence on the behavior of the hybrid system, but the properties of the composite hybrid films are different from their parent components.

4. Conclusions

In this paper we have described the synthesis of new polymeric organic–inorganic hybrid compounds based on silica and a polyelectrolyte complex between CHI and PMMI, which are very interesting, since materials with high functionality can be obtained with different properties from those of the starting materials but with the advantage of preserving the inherent property of each component. The introduction of the organic groups in the inorganic network leads to new structural properties and therefore promotes new applications for the resulting composite material such as functional coating by introducing ions and/or small molecules.

The products can be prepared as self-supported homogeneous and transparent films or deposited as well adhering coatings on a variety of surfaces. Intermolecular hydrogen bonding probably stabilizes this self-assembled structure. PMMI and SiO_2 do not form a polymeric hybrid, however as a consequence of the interaction generated with CHI the compatibility between the PMMI and silica gel was improved generating dispersion at the molecular level. Chitosan acts as a linker between PMMI and SiO_2. Morphological and spectroscopic studies revealed the nanometer dimension of each phase. Also it's possible to control the concentration of amino and carboxylic groups in the films and thereafter change its ionic properties by varying the composition of the organic components. These properties will be examined in future works. Due to their adhering properties, the prepared films already imply a use as pH responsive transparent coatings. Also, their

transformation to mesoporous silica films may bear potential for new material applications of mesoporous silica apart from the standard silica templating of lyotropic phases.

In addition, the described hybrid films with a high amount of amine groups with respect to carboxyl groups, with adjustable protonation degree via a simple pH variation, are also promising candidates for the incorporation of functional inorganic particles like semiconductors or magnetic particles. As the films are stable over an extended pH range (pH 4–9), the mineral-film interaction can be adjusted by simple pH variation so that a large variety of inorganic particles can be potentially precipitated inside these films. The use of gel structures for the precipitation of magnetite was already demonstrated [33] so that the combination of the adhering properties of the reported films and their optical transparency with their further functionalization with inorganic particles may lead to new interesting functional materials.

Acknowledgements

This work was partially supported by CONICYT (Projects Fondecyt 1010525 and Fondap 1198000-2). Y. M. thanks Deutscher Akademischerr Austauschdienst (DAAD) for a doctoral fellowship. H.C. thanks the Max-Planck-Society for partial financial support of this work.

References

[1] Chujo Y, Saegusa T. Adv Polym Sci 1992;100:11.
[2] Corriu RJP, Leclercq D. Angw Chem, Int Ed 1996;35:1420.
[3] Judeinstein P, Sanchez C. J Mater Chem 1996;6:511.
[4] Arenas LT, Aguirre TAS, Langaro A, Gushikem Y, Benvenutti EV, Costa TMH. Polymer 2003;44:5521.
[5] Schottne G. Chem Mater (Rev) 2001;13:3422.
[6] Chan CK, Peng SL, Chu I, Ni SC. Polymer 2001;42:4186.
[7] Mitzi DB. Chem Mater 2001;13:3283.
[8] Collinson MM, Howells AR. Anal Chem 2000;702.
[9] Sánchez C, Ribot F, Lebeau B. J Mater Chem 1999;9:35.
[10] Loy DA. MRS Bull 2001;26:364.
[11] Retuert J, Nuñez A, Martínez F. Macromol Rapid Commun 1997;18:163.
[12] Peniche C, Elvira C, San Roman J. Polymer 1998;39:6549.
[13] Peniche C, Arguelles-Monal W, Davidenko N, Sastre R, Gallardo A, San Roman J. Biomaterials 1999;20:11869.
[14] Kim SG, Kim Y, Jegal J, Lim G, Lee K. J Appl Polym Sci 2002;85:714.
[15] Rinaudo M, Domard A. Chitin and chitosan: sources, chemistry, physical properties and applications. Essex, UK: Elsevier Science Publishers; 1989. p. 71.
[16] Baker BR, Shaub RE, Wiliams GH. J Org Chem 1952;17:122.
[17] Pope EJA, Mackenzie JD. J Non-Cryst Solids 1988;101:198.
[18] Arguelles W, Peniche C. Macromol Rapid Commun 1988;9:693.
[19] Jang J, Park H. J Appl Polym Sci 2002;83:1817.
[20] Wang H, Li W, Lu Y, Wang Z. J Appl Polym Sci 1997;65:1445.
[21] Barraza RG, Ríos H. Polym Int 1995;38:387.
[22] Manning GS. J Phys Chem 1975;79:262.
[23] Muzzarelli RAA. Chitin. Oxford: Pergamon Press; 1977. p. 103.
[24] Pérez-Gramatges A, Arguelles W, Peniche C. Polym Bull 1996;37:127.
[25] Yazdani-Pedram M, Calderon K, Quijada R. Bol Soc Chil Quím 2000;45:269.
[26] Arguelles W, Gárciga M, Peniche C. Polym Bull 1990;23:307.
[27] Zoppi RA, Garcia C. Adv Polym Tech 2002;21:2.
[28] Chujo Y, Motsuki H, Kure S, Saegnsa T, Yazawa T. J Chem Soc Chem Commun 1994;635.
[29] Wei Y, Xu J, Dong H, Dong JH, Qiu K, Jansen-Varnum SA. Chem Mater 1999;11:2023.
[30] Sakiyama T, Takata H, Kikuchi M, Nakanishi K. J Appl Polym Sci 1999;73:2227.
[31] Schröder UP, Oppermann W. Properties of polyelectrolyte gels. In: Cohen Addad JP, editor. Physical properties of polymer gels. New York: Wiley; 1996. p. 19.
[32] Yazdani-Pedram M, Quijada R. J Macromol Chem Phys 2000;201:923.
[33] Breulmann M, Cölfen H, Hentze HP, Antonietti M, Walsh D, Mann S. Adv Mater 1998;10:237.